Mechanical interaction of the egg parasitoid *Anastatus bifasciatus* (Hymenoptera: Eupelmidae) with artificial substrates and its host egg

Manuela Rebora[1], Gianandrea Salerno[2]*, Silvana Piersanti[1], Valerio Saitta[2], Elena Gorb[3] and Stanislav N. Gorb[3]

[1]Dipartimento di Chimica, Biologia e Biotecnologie, University of Perugia, Perugia, Italy, [2]Dipartimento di Scienze Agrarie, Alimentari e Ambientali, University of Perugia, Perugia, Italy, [3]Department of Functional Morphology and Biomechanics, Zoological Institute, Kiel University, Kiel, Germany

Egg parasitoids play an important role in biological control of pest species attacking and killing their hosts at an early stage of their development. During the antagonistic coevolution with their hosts, egg parasitoids have developed a great ability to locate their host using chemical cues. A considerable amount of literature is available on this topic, while nothing is known about a possible adaptation of egg parasitoids to topography and mechanical properties of egg surface features and its shape when attaching to the host egg for oviposition. In the present investigation, the attachment ability of adults of both sexes of the egg parasitoid *Anastatus bifasciatus* (Hymenoptera: Eupelmidae) to artificial (polishing paper, flat glass, glass beads as dummies of the host egg) and natural surfaces (eggs of *Halyomorpha halys* and *Nezara viridula*, both Heteroptera: Pentatomidae), with different roughness and wettability, was measured using centrifugal force tester and traction force experiments. The parasitoid attachment devices and the egg surfaces were examined under cryo scanning electron microscope, wettability and roughness of natural and artificial substrates were characterised. We detected differences in the attachment devices and attachment ability of the two sexes. The collected data revealed a special ability of the female to attach to the eggs of the host species, thus suggesting an adaptation of the *A. bifasciatus* female to the surface features of the eggs during oviposition.

Introduction

Egg parasitoids attack eggs of many arthropod species and play an important role in the biological control of pest species (van Lenteren et al., 2018). The host embryo is killed and the immature wasp feeds on it until its emergence.

Host location to parasitize suitable hosts is a complex process in egg parasitoids, encompassing host habitat location, host location, and host acceptance, which are completed with the oviposition in the host egg. This process is mediated by numerous stimuli, among which chemicals are known to play a major role (Vinson, 1998; Conti and Colazza, 2012). During coevolution with their hosts, egg parasitoids have developed a great ability to locate their host using highly detectable long-range and short-range chemical cues, especially oviposition-induced plant volatiles and odours of host gravid females, males and nymphs (Hilker and Meiners, 2006; Fatouros et al., 2008; Chiappini et al., 2012; Conti and Colazza, 2012; Peri et al., 2013; Hilker and Fatouros, 2015). A considerable amount of literature is available on this topic while less is known about a possible adaptation of egg parasitoids to the surface features of the egg when attaching to the host egg for oviposition. Owing to their small dimensions and the frequent oviposition in egg clutches, typically many egg parasitoid species walk on the egg surface of the host insect before egg-laying (e.g., *Trichogramma* sp. in Schmidt and Smith, 1985). This is to "taste" the chemicals present on the chorion surface, but also to evaluate its size (see review in Schmidt, 1991). Before oviposition, the wasp examines the host surface by walking over it, turning at the edge, and "drumming" with its antennae (Schmidt and Smith, 1985). The mechanical inspection of the host egg and its size evaluation is important because whereas polyphagous egg parasitoid wasps can accept a broad range of host size, oligophagous parasitoids, such as *Telenomus heliothidis* Ashmead (Hymenoptera: Scelionidae), restrict host acceptance to a small range of host sizes (Strand and Vinson, 1983). For gregarious egg parasitoids, such as species from the genus *Trichogramma,* it is extremely important to evaluate the egg size for offspring survival (Salt, 1958).

Efficient attachment devices are necessary for the parasitoid wasp to walk on the egg, adhere to the egg chorion, and lay eggs, exactly as for a phytophagous insect in the case of a host plant. The need to firmly adhere with the legs to the egg surface is particularly relevant when the female unsheathes the ovipositor and points it toward the substrate to insert it into the egg chorion. On the other hand, insect eggs like plants cannot defend themselves actively by escaping from the attack of predators and parasitoids. Some insect species can defend their eggs from egg parasitoids using different strategies, such as a safe hidden oviposition site, egg chorion resemblance to plant structures, water droplets, disruptive colouration, special secretions from accessory glands, chorion surface special covering or egg toxins (see review in Fatouros et al., 2020), but many species are exploited by egg parasitoids. The insect orders escaping egg parasitism contain only about 30% of the total number of estimated insect species (Fatouros et al., 2020). In all other insect species, whose eggs are exploited by parasitoids, we hypothesize possible antagonistic coevolution between insect attachment devices and chorion surface features, exactly as in the antagonistic evolution between phytophagous insect attachment devices and plants' surface features (see review in Gorb and Gorb, 2013). This could lead to special adaptations in the attachment ability of egg parasitoids, especially in females, which are challenged by egg-laying behaviour.

Anastatus bifasciatus (Geoffroy) (Hymenoptera: Eupelmidae) can attack eggs of more than 30 host species belonging to Heteroptera and Lepidoptera (Noyes, 2019) and thus can be considered a polyphagous egg parasitoid (Stahl et al., 2018). In Europe, this species represents the most important native egg parasitoid of the eggs of the highly invasive pest species *Halyomorpha halys* Stål (Hemiptera: Pentatomidae), the brown marmorated stink bug (Roversi et al., 2016; Stahl et al., 2019; Moraglio et al., 2020; Andreadis et al., 2021), but can attack also other Pentatomidae species, such as the southern green stink bug *Nezara viridula* L. (Hemiptera: Pentatomidae) (Stahl et al., 2018). It lays one single egg in each parasitized host egg (Stahl et al., 2019). The egg size of the host is an important parameter for the egg parasitoid since its sex ratio and female size are strictly related to this (Stahl et al., 2018).

In the present investigation, we tested the hypothesis of a possible antagonistic coevolution between egg parasitoid attachment devices and chorion surface features, potentially leading to special adaptations in the attachment ability of egg parasitoid females. We compared the attachment ability of this parasitoid species in relation to the surface features of the substrate with that recorded in other insect species and verified the presence of sexual dimorphism of this egg parasitoid species in the attachment ability to natural and artificial surfaces. In particular, the attachment ability of adults of both sexes of the egg parasitoid *A. bifasciatus* to artificial and natural surfaces (eggs of *H. halys* and *N. viridula*) with different roughness and wettability properties was measured using a centrifugal force tester and traction force experiments. The parasitoid attachment devices (pretarsal attachment devices), the tarsi and the egg surface of the two hosts were examined under a cryo scanning electron microscope (cryo-SEM), wettability and roughness of natural and artificial substrates were characterised. Also, some behavioural observations on egg-laying females were performed.

Material and methods

Insects

Adults of *A. bifasciatus* of both sexes were supplied by the commercial insectary Bioplanet, Cesena, Italy. Insects were

maintained in the laboratory in vials in an environmental chamber (14 h photoperiod, temperature of 23°C ± 1°C, and relative humidity of 60% ± 10%) and were fed with small drops of honey on plastic strips. Adults of both sexes were used in the experiments. Ten females and ten males of *A. bifasciatus* were weighted with the Sartorius MSE2.7S ultra microbalance.

Eggs of *H. halys* were supplied by the commercial insectary Bioplanet, Cesena, Italy. Eggs of *N. viridula* were obtained from insects reared in the laboratory of the Department of Scienze Agrarie, Alimentari e Ambientali of the University of Perugia (Italy). *N. viridula* was reared in an environmental chamber (14 h photophase, temperature of 25°C ± 1°C; RH of 70% ± 10%) inside net cages (300 mm × 300 mm × 300 mm) (Vermandel, Hulst, Netherlands). Sunflower [*Helianthus annus* L. (Asteraceae)] seeds, pods of French bean [*Phaseolus vulgaris* L. (Fabaceae)] and cabbage [*Brassica oleracea* L. (Brassicaceae)] leaves were used to feed nymphs and adults.

Light microscopy

To measure the arolium width, the pretarsi of dried specimens of both sexes were soaked in a 5% solution of lactic acid for 24 h to promote arolium expansion (Gladun and Gumovsky, 2006). The soaked pretarsi with spread arolia were then washed in water and fixed in 5% glutaraldehyde solution for 10–15 min, rinsed in water and subsequently mounted in glycerine. Arolia were observed and photographed with a microscope Leika DMLB connected to a Koppace FHD Camera V 2.0. Pictures were analysed using the software ImageJ (Sun-Java, United States). Legs of *A. bifasciatus* males and females were observed and photographed with the same microscope and camera.

Cryo scanning electron microscopy

The tarsi together with the pretarsal attachment devices (arolium and claws) of both sexes of *A. bifasciatus* and the eggs of *H. halys* and *N. viridula* were studied in a scanning electron microscope (SEM) Hitachi S-4800 (Hitachi High-Technologies Corp., Tokyo, Japan), equipped with a Gatan ALTO 2500 cryo-preparation system (Gatan Inc., Abingdon, United Kingdom). For details of sample preparation and mounting for cryo-SEM, see Gorb and Gorb (2009). Whole mounts of insect tarsi and eggs were sputter-coated in frozen conditions with gold-palladium (thickness 10 nm) and examined at 3 kV acceleration voltage and temperature of −120°C at the cryo-stage within the microscope.

Behavioural observations

The behaviour of the female of *A. bifasciatus* ovipositing on eggs of *H. halys* has been observed and recorded using a stereomicroscope Leica MZ6 connected to a high-speed camera Imaging source DMK37BUX287. Three egg-laying females were observed and each one was recorded ovipositing on at least five individual eggs. The portion of the tarsi of forelegs, midlegd and hindlegs in contact with the egg chorion during the different oviposition steps was observed.

Preparation and characterization of the tested substrates

Artificial substrates represented by polishing paper with different asperity sizes (average diameter of the abrasive particles −0.3, 1, 3, 9, 12, 35 and 125 μm) and glass with different wettability [hydrophobic glass with a water contact angle of 112.62 ± 3.13° (mean ± SD) and hydrophilic glass with a water contact angle of 32.49 ± 4.17° (mean ± SD)] were used in the centrifugal force tester experiments. Hydrophobic glass has been prepared by treatment of a glass plate by vapour phase deposition silanization method using dichlorodimethyl-silane. A glass disk was rinsed and sonicated in an ultrasound bath (Bandelin electronic, Berlin, Germany) for 5 min with ethanol (70%) and distilled water. This was repeated several times and remained liquid on the substrate was blown by compressed air. Cleaned glass was subjected to air plasma treatment (Diener electronic, Ebhausen, Germany) and then it was vacuum pumped (BÜCHI Labortechnik, Flawil, Switzerland) in a desiccator together with a glass vial containing 200 μl of dichlorodimethylsilane (Merck Schuchardt, Hohenbrunn, Germany). The vacuum pump was disconnected from the desiccator once the silane started to boil, and the desiccator was left closed for 5 h to achieve sufficient deposition of the silane on the glass. The surface-modified glass was rinsed thoroughly with isopropanol and distilled water and was blown dry by compressed air.

In the Biopac force tester experiments, a series of artificial substrates mimicking the host insect egg clutches were prepared using glass beads having different diameters (0.53 ± 0.03, 0.85 ± 0.02, 1.35 ± 0.02, 1.98 ± 0.04, and 3.06 ± 0.01 mm) and a water contact angle of 92.02 ± 1.03° (mean ± SD). Similar substrates as glass dummies of the host eggs were used in other behavioural investigations (Conti et al., 2003). Groups of glass beads with the same diameter were glued (Super Attack, Loctite Henkel Adhesives, Düsseldorf, Germany) on a glass microscope slide forming a single layer to mimic an egg clutch. An untreated microscope slide was used as flat hydrophilic glass substrate [water contact angle of 27.02 ± 0.64° (mean ± SD)].
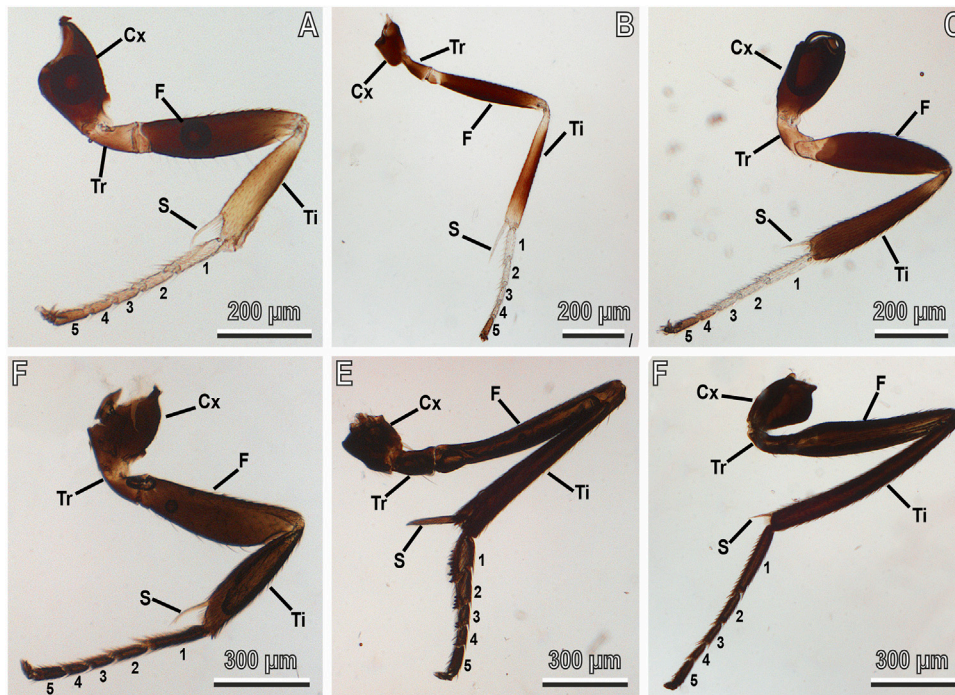
FIGURE 1
Legs of *A. bifasciatus*, light microscopy. Male foreleg **(A)**, midleg **(B)** and hindleg **(C)**; Female foreleg **(D)**, midleg **(E)** and hindleg **(F)**. Tarsi of both sexes are composed of five tarsomeres (1–5). Note **(E)** that in the female, the tarsi of the medium legs have a curved shape and the first tarsomere (1) is wider than the others. Cx, coxa; F, femur; Ti, tibia; Tr, trochanter; S, tibial spur.

The roughness of different polishing paper with asperity sizes of 0.3, 1, 3, 9, 12, 35 and 125 μm was characterized using the white light interferometer (Salerno et al., 2017). Roughness data are reported in Salerno et al. (2022).

The wettability of surfaces used in the experiments (smooth hydrophilic glass, smooth hydrophobic glass, glass beads, eggs of *H. halys* and *N. viridula*) was characterized by determining the contact angles of water (aqua millipore, droplet size: 1 μl for glass substrate and 0.5 μl for glass beads and eggs, sessile drop method) using a high-speed optical contact angle measuring instrument OCAH 200 (Dataphysics Instruments GmbH, Filderstadt, Germany). Ten measurements (*n* = 10) were performed for each substrate.
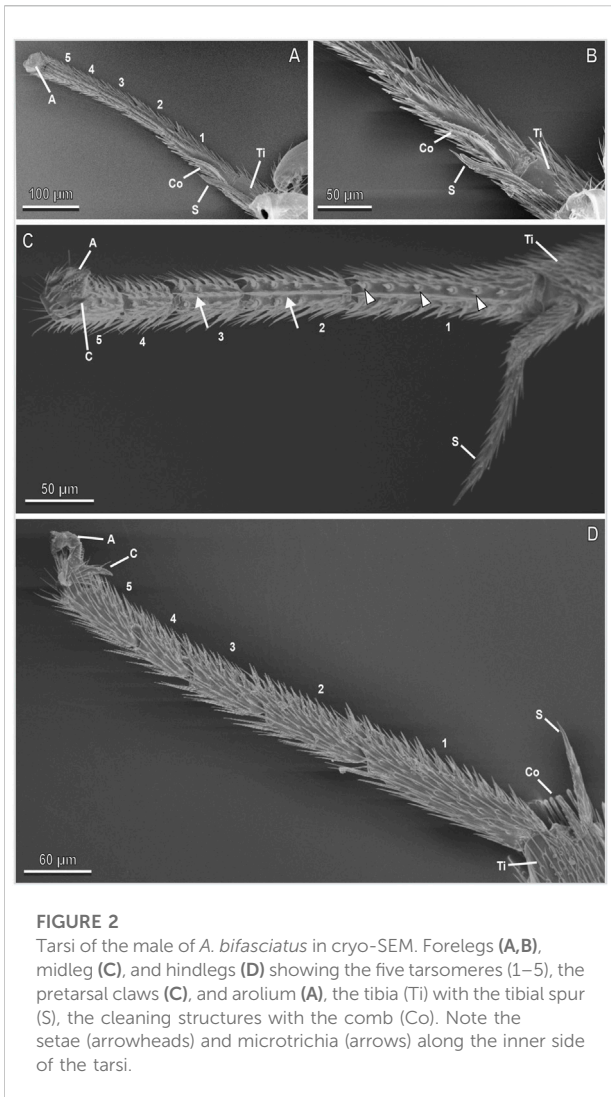
Centrifugal force tester experiments

To test the attachment ability of *A. bifasciatus* to artificial substrates represented by polishing paper with different asperity sizes and flat hydrophilic and hydrophobic glass, a centrifugal force tester (Gorb et al., 2001) was used. Males were not tested on polishing paper with 35 and 125 μm asperity sizes because, due to their small dimension, the optic sensor could not detect them on these rough surfaces.

The centrifuge is constituted of a metal drum covered by a substrate disc to be tested. The metal drum is driven by a computer-controlled motor. Just above the disc, the fibre-optic sensor monitored by the computer is placed. After positioning the insect on the horizontal disc, the centrifuge drum was allowed to begin the rotation at a speed of 50 rev min^{-1} (0.883 rev s^{-1}). The position of the insect on the drum was monitored by using a combination of a focused light beam and a fibre-optical sensor. The drum speed was continuously increased until the insect lost its hold on the surface under centrifugal force. The rotational speed at contact loss, the last position of the insect on the drum (radius of rotation), and the insect weight were used to calculate the maximum frictional component of the attachment force. In total, 38 females and 25 males of *A. bifasciatus* were tested. In random order, each specimen was tested on four or five different surfaces and on hydrophilic glass as a reference.

Biopac force tester experiments

This force measuring experimental set-up was used for testing the insect attachment ability to artificial substrates with glass beads of different sizes, eggs of *H. halys* and *N.*

FIGURE 2
Tarsi of the male of *A. bifasciatus* in cryo-SEM. Forelegs **(A,B)**, midleg **(C)**, and hindlegs **(D)** showing the five tarsomeres (1–5), the pretarsal claws **(C)**, and arolium **(A)**, the tibia (Ti) with the tibial spur (S), the cleaning structures with the comb (Co). Note the setae (arrowheads) and microtrichia (arrows) along the inner side of the tarsi.

AcqKnowledge 5.0 software (Biopac Systems Ltd., Goleta, CA, United States). Pull-off force values were estimated using the force-time curves as the maximum of the detected forces. 30 females and nine males were tested.

Statistical analysis

The friction force of *A. bifasciatus* on polishing paper with different asperity sizes normalised to the insect friction force recorded on smooth hydrophilic glass was analysed separately for females and males using the one-way analysis of variance (ANOVA). For data obtained on polishing paper with asperity sizes of 0.3, 1, 3, 9, and 12 μm, the male and female normalised friction forces were compared using the Student t-test for independent samples.

The comparisons of the safety factor (the force divided by the insect weight) and force values of *A. bifasciatus* females and males on smooth hydrophilic and hydrophobic glass (friction force) as well as on eggs of *H. halys* and *N. viridula* (pull-off force) were conducted using the repeated measures analysis of variance (ANOVA) considering the insect sex as a factor.

The safety factor and pull-off force of *A. bifasciatus* females and males on a flat glass surface and glass beads with different diameters were analysed using the two-way analysis of variance (ANOVA), considering the insect sex and the different substrates as factors. Before the analysis, the data were subjected to Box-Cox transformations, to reduce data heteroscedasticity (Sokal and Rohlf, 1998).

Data on arolium width of forelegs, midlegs and hindlegs in males and females of *A. bifasciatus* were analysed using the two-way analysis of variance (ANOVA), considering the insect sex and different legs as factors.

The ANOVA analyses were followed by the Tukey unequal N HSD post hoc test for multiple comparisons between means (Statistica 6.0, Statsoft Inc., 2001).

Results

Tarsal and pretarsal morphology of *A. bifasciatus* adults and oviposition behaviour

The tarsi of *A. bifasciatus* are composed of five tarsomeres and show sexual dimorphism, especially in the midlegs (Figure 1). These last have straight tarsi in the male and all tarsomeres have the same width, while in the female the tarsi of the medium legs show a curved shape and the first tarsomere is wider than the others (Figure 1). Observations under cryo-SEM reveal that the forelegs and hindleg tarsi in males (Figures 2A,B,D) and females (Figure 3) are similar and show no special differentiation except for a cleaning structure (comb) located in the proximal portion of the forelegs (Figures 2A,B, 3A,C).

viridula and flat hydrophilic glass. Forces were measured with the load cell force sensor FORT-10 (10 g capacity; World Precision Instruments Inc., Sarasota, FL, United States) connected to a force transducer MP 160 (Biopac Systems Ltd., Goleta, CA, United States) (Gorb et al., 2010). The sensor was kept in the horizontal position and the insect thorax was attached using a small drop of glue (Super Attack, Loctite Henkel Adhesives, Düsseldorf, Germany) to the tip of a vertical pin fixed to the sensor. Experimental insects were anaesthetized with carbon dioxide for 60 s before gluing their thorax to the pin and allowed to recover undisturbed for 5 min before testing them. The force sensor was fixed to a motorised micromanipulator (Narishige MMO-203) and moved in such a way that the insect was in contact with all six legs to the tested surface. Afterwards, the force sensor was moved in a direction perpendicular to the surface until the insect detached from it. Data were recorded using

FIGURE 3
Tarsi of the female of *A. bifasciatus* in cryo-SEM. Forelegs **(A−C)** and hindlegs **(D,E)** showing the five tarsomeres (1−5), the pretarsal claws (C) and arolium (A), the tibia (Ti) with the tibial spur (S), the cleaning structures with the comb (Co) and the spatulate setae (SS). Note the setae (arrowheads) and microtrichia (arrows) along the inner side of the tarsi.

Articulated setae and microtrichia are visible on the inner side of the tarsi (Figures 2C, 3B,E) and spurs (S) are present at the distal tibia in all the legs of both sexes (Figures 1–3). The tarsi of the midleg in the male show setae (arrowheads in Figure 2) and microtrichia (arrows in Figure 2) along their inner side (Figure 2C), whereas in the female midleg tarsi the inner side of each tarsomere is characterised by a central row of microtrichia and two lateral rows of big and thick pegs, which are set one close to the other (Figures 4A–F). The pegs are articulated, pointed in their apical portion and slightly curved towards the inner portion of the tarsomere, with longitudinal grooves. They are about ten in the first tarsomere forming two rows facing one to the other, about eight in the second tarsomere, four in the third one, and two in the fourth one, while no peg is present in the last tarsomere (Figure 4B). In the first and second tarsomeres hosting the higher number of pegs, there are more pegs in the posterior row than in the anterior one (Figures 4C,D).

The pretarsal attachment devices of *A. bifasciatus* are similar in both sexes and are constituted of a smooth pad, the arolium (A) and a pair of claws (C) (Figure 5). The arolium dorsally is articulated to the fifth tarsomere through the manubrium (MA), a subtriangular sclerite with five or six long hairs along its distal margin and one distal hair (DH) (Figures 5A,B,D). The arolium is supported by dorsal sclerites named dorsal plates (DP) in continuity with the arcus (ARC) surrounding the arolium proximally and ventrally (Figures 5A–D). The arolium can be

inverted and nearly invisible (Figures 5E,F) or everted [completely (Figures 5B–D) or partly spread (Figure 5A)]. When the arolium is everted, it is formed by two big lobes separated by a dorsal deep median cleft (Figures 5B–D). The surface of the everted arolium is not smooth but wrinkled (Figure 5C). Ventrally a quadrangular unguitractor plate (UP) with microtrichia and scales along with its lateral surface inserts into the last tarsomere and is in continuity with planta (P), whose distal portion extends in the arolium (Figure 5F). Two claws covered with some setae are located laterally to the hairy planta (Figure 5F). When the arolium is everted, the claws are rotated towards the last tarsomere (Figures 5C,D). When the arolium is inverted, the claws are kept along the hairy planta (Figure 5F).

The female weight is 0.52 ± 0.04 mg ($n = 16$) and the male weight is 0.30 ± 0.02 mg ($n = 15$). The arolium width was greater in females compared to males, but not statistically different among forelegs (males: 183.4 ± 3.6 µm; females: 214.7 ± 4.6 µm), midlegs (males: 167.1 ± 6.7 µm; females: 218.1 ± 6.8 µm) and hindlegs (males: 188.7 ± 7.2 µm; females: 218.9 ± 4.0 µm) (legs: $F = 1.9$; d.f. $= 2$, 102; $p = 0.15$; sex: $F = 65.6$; d.f. $= 1$, 102; $p < 0.001$; legs x sex: $F = 2.1$; d.f. $= 2$, 102; $p = 0.12$).

Behavioural observations of the egg-laying females on the eggs of *H. halys* (Figure 6) revealed that during oviposition, the female touches the egg chorion with the tarsal tip of the fore- and hindlegs. In these legs, the females use only the pretarsal attachment devices
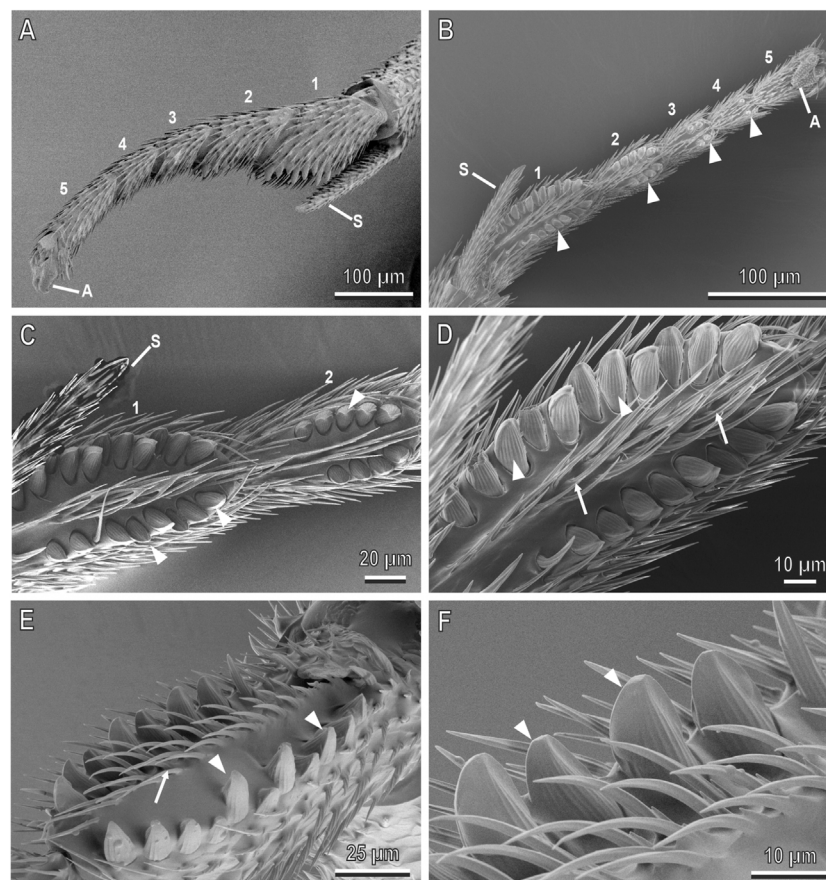
FIGURE 4
Midleg tarsi of the female of *A. bifasciatus* in cryo-SEM. **(A)**, Lateral view of the tarsus showing five curved tarsomeres (1–5) with the first tarsomere wider than the others; **(B)**, Ventral view of the tarsus showing the two lateral rows of big and thick pegs (arrowheads); **(C,D)**, Detail of **(B)** showing the first and second tarsomeres with the two rows of articulated pegs (arrowheads) surrounding a row of setae (arrows); **(E,F)**, Details showing the pegs (arrowheads) slightly curved towards the inner portion of the tarsomere, with longitudinal grooves. Pegs are surrounded by setae (arrows). A, arolium; S, tibial spur.

(claws and arolium) to attach to the egg surface and the tarsi are not contacting the egg. Conversely in the midlegs, the ventral surface of the whole tarsus is in close contact with the chorion. The contact of the thick pegs located on the first four tarsomeres with the egg surface is clearly visible (Figure 6D and inset). The developed tibial spur of the midlegs is in contact with the egg surface and forms a wide angle with the tarsus (Figure 6).

Host egg morphology and wettability

The egg clutches of *H. halys* consist of about 27–28 eggs. Each egg is light green or light blue, has a subspherical shape and a diameter of 1.28 ± 0.01 mm (mean ± SE) (Figure 7A). A crown of aeromicropilar processes is located along the apical egg surface (Figure 7B). The whole chorion surface is rough due to wrinkles and tubercles (Figure 7C). The egg clutches of *N. viridula* are

constituted of about 30–130 eggs. The eggs are cream to yellow in colour and barrel-shaped, with flat tops and a diameter of 0.82 ± 0.01 mm (mean ± SE) (Figures 7D–F). A crown of aeromicropilar processes (processes with a central channel for the sperm passage and respiratory exchange in many Heteroptera species) is present along the apical surface (Figure 7E). The chorion is smooth, with some rough areas around the aeromicropiles (Figure 7F).

The contact angle of water to the eggs of *H. halys* is 134.9 ± 4.3° (mean ± SE, $n = 10$) and that to *N. viridula* eggs is 120.6 ± 1.3° (mean ± SE, $n = 15$).

Attachment ability of *A. bifasciatus* to rough surfaces

In the centrifugal experiments on polishing paper with different asperity size (0.3, 1, 3, 9, 12, 35 and 125 μm; 35 and
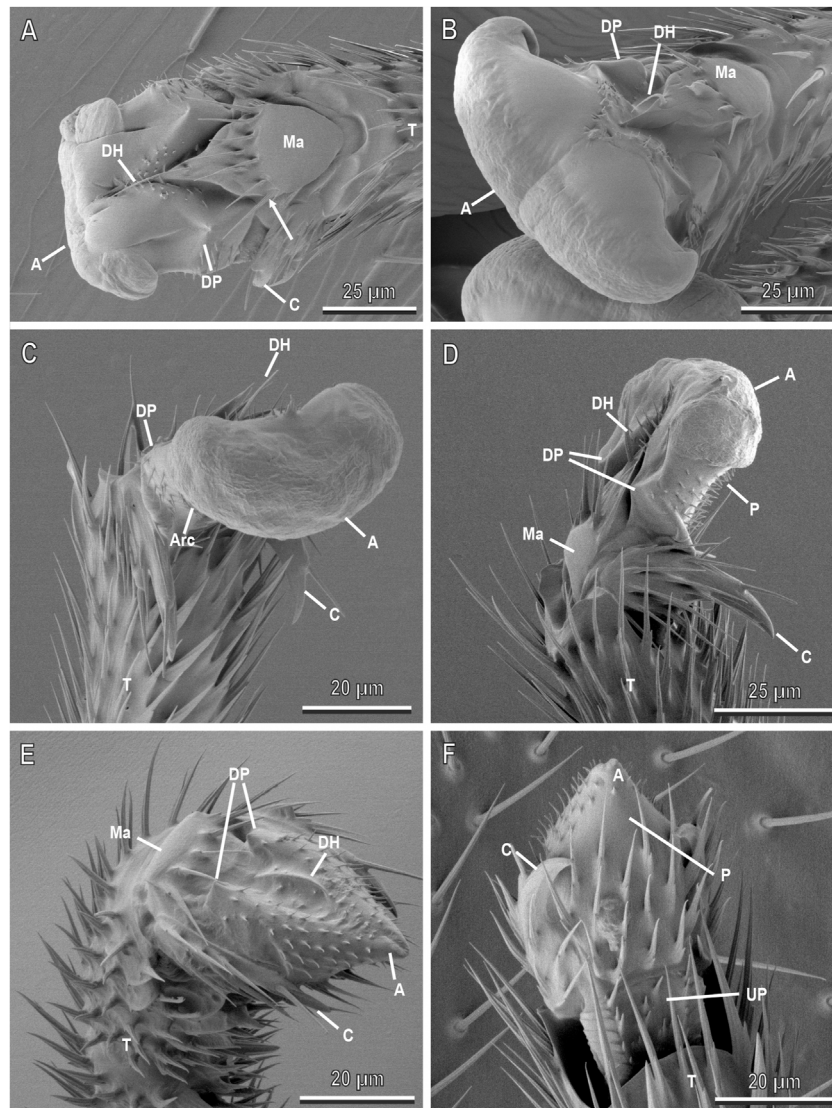
FIGURE 5
Pretarsal attachment devices of *A. bifasciatus* in cryo-SEM. **(A)**, Dorsal view of the female pretarsus showing the partially everted arolium **(A)** articulated to the fifth tarsomere (T) through the manubrium (Ma) with 5–6 long hairs (arrow) and one distal hair (DH). The arolium is supported by dorsal sclerites named dorsal plates (DP) in continuity with the arcus surrounding the arolium proximally and ventrally; **(B)**, Dorsal view of the female pretarsus with the everted arolium formed by two big lobes separated by a dorsal deep median cleft; **(C)**, Latero-frontal view of the male pretarsus with the everted arolium. The dorsal plates are in continuity with the arcus (Arc) surrounding the arolium proximally and ventrally. Note the wrinkled surface; **(D)**, Lateral view of the male pretarsus with the everted arolium; **(E)**, Latero-frontal view of the male pretarsus with the inverted arolium; **(F)**, Ventral view of the male pretarsus with the inverted arolium in continuity with the planta (P) connected to the quadrangular unguitractor plate (UP) with microtrichia and scales. C, claws.

125 μm tested only in females) (Figure 8), normalised friction force (normalised to friction force recorded on hydrophilic glass as reference) of females was significantly higher than that of males on all the tested surfaces (0.3 μm: $t = 4.0$; d.f. = 28; $p < 0.001$; 1 μm: $t = 3.4$; d.f. = 28; $p = 0.002$; 3 μm: $t = 2.8$; d.f. = 28; $p = 0.010$; 9 μm: $t = 3.1$; d.f. = 28; $p = 0.005$; 12 μm: $t = 2.9$; d.f. = 28; $p = 0.008$). In females, the force on the surface with the intermediate asperity size

(9 μm) was significantly higher than that recorded on surfaces with the smallest (0.3 and 1 μm) and highest roughness, such as 35 and 125 μm, while the force values on surfaces with asperity size 3 and 12 μm was intermediate ($F = 3.8$; d.f. = 6, 98; $p = 0.002$). In males, the force was not significantly different on surfaces with asperity sizes 3, 9, and 12 μm and significantly higher compared to the force on 0.3 μm surface. On the surface with an asperity size of 1 μm,
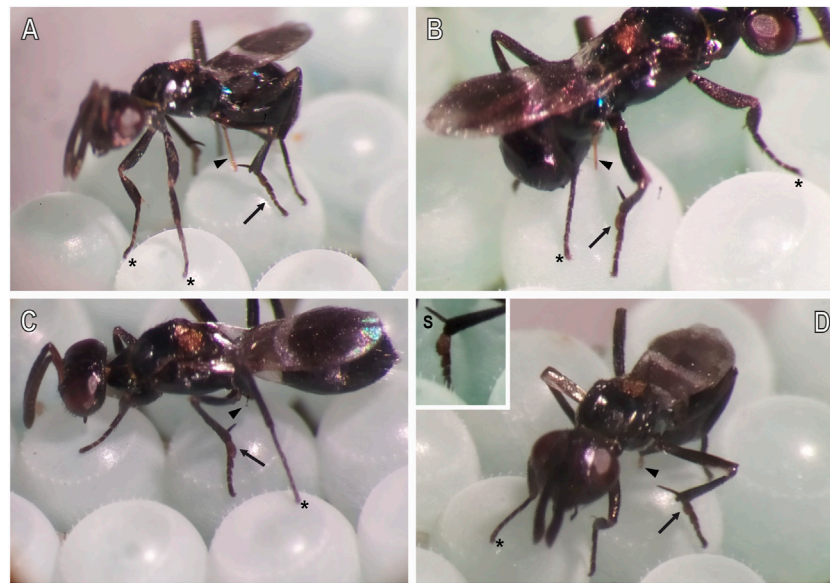
FIGURE 6
Interaction between the tarsi of egg-laying females of *A. bifasciatus* and the egg surface of *H. halys* observed with the stereomicroscope. **(A–C)**, Different steps during oviposition up to the insertion of the ovipositor (arrowhead) into the egg [**(D)** and inset]. Note that forelegs and hindlegs (marked with asterisk) are in contact with the egg chorion only through the tarsal tip and the pretarsal attachment devices (claws and arolium), while in the midlegs the ventral surface of the whole tarsus (arrow) is in close contact with the chorion. In the midlegs, the tibial spur (S) is contacting the egg surface and forms a wide angle with the tarsus.

the force value was intermediate ($F = 4.1$; d.f. = 4, 70; $p = 0.005$).

Attachment ability of *A. bifasciatus* to hydrophilic and hydrophobic surfaces

There is no significant difference between the force of males and females on both hydrophilic and hydrophobic surfaces. The attachment ability of females does not differ on both surfaces, while the friction force of males is significantly higher on hydrophilic glass than on hydrophobic glass (sex: $F = 0.5$; d.f. = 1, 28; $p = 0.473$; surfaces: $F = 13.9$; d.f. = 1, 28; $p < 0.001$; sex x surf.: $F = 6.8$; d.f. = 1, 28; $p = 0.015$) (Figure 9A).

On the smooth hydrophilic glass, the safety factor of males is significantly higher than that of females, while there is no significant difference between the safety factor of males and females on smooth hydrophobic glass (Figure 9B). In females, difference between the safety factors on hydrophilic glass and hydrophobic glass is non-significant, while males attach significantly stronger to hydrophilic glass than to hydrophobic glass (Figure 9B) (sex: $F = 32.9$; d.f. = 1, 28; $p < 0.001$; surfaces: $F = 19.3$; d.f. = 1, 28; $p < 0.001$; sex x surf.: $F = 12.7$; d.f. = 1, 28; $p = 0.001$).

Attachment ability of *A. bifasciatus* to glass beads of different sizes

In the Biopac force tester experiments with artificial substrates bearing glass beads with different diameters used as dummies of the host eggs, the force values in females are significantly higher than those in males on surfaces constituted of beads with a diameter of 0.5, 0.9 and 1.4 mm, while there is no significant difference between males and females on the surfaces bearing 2.0 and 3.1 mm beads and on smooth glass (Figure 10A). In females, the forces are significantly higher on the surfaces composed of beads with a diameter of 0.5, 0.9 and 1.4 mm compared to the surfaces constituted of 2.0 and 3.1 mm beads. The force values on these last surfaces are higher than that recorded on flat glass (Figure 10A). In males, the forces are significantly higher on the surfaces constituted of beads with a diameter of 0.5, 0.9 and 1.4 mm than on flat glass, while on surfaces with 2.0 and 3.1 mm beads it is intermediate (Figure 10A) (sex: $F = 94.6$; d.f. = 1, 128; $p < 0.001$; surfaces: $F = 28.1$; d.f. = 5, 128; $p < 0.001$; sex x surf.: $F = 2.3$; d.f. = 5, 128; $p = 0.049$).

As for the safety factor, there is no significant difference between males and females for each tested surface (Figure 10B). In females, the safety factor is significantly higher on the surfaces constituted of beads with a diameter of 0.5, 0.9 and 1.4 mm compared to the surfaces with beads of
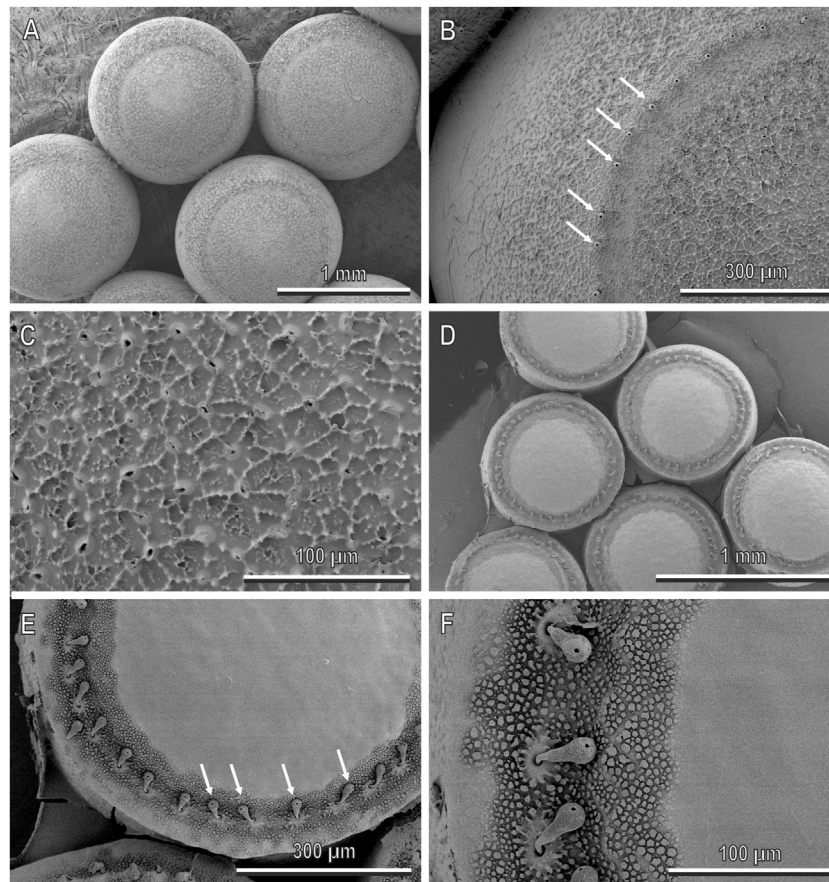
FIGURE 7
Eggs of *H. halys* **(A–C)** and *N. viridula* **(D–F)** in cryo-SEM, dorsal view. **(A,D)**, Egg clutches. Each egg of *H. halys* has a subspherical shape **(A)**, rough surface **(C)** and crown of aeromicropilar processes along the apical egg surface (arrows) **(B)**. Each egg of *N. viridula* has a barrel shape with a flat top **(D)**, smooth surface **(E,F)** and crown of aeromicropilar processes (arrows) located along the apical surface **(E)**.

2.0 and 3.1 mm in diameter. The safety factor on these last surfaces is higher than that recorded on flat glass (Figure 10B). In males, the safety factor is significantly higher on the surfaces constituted of beads with a diameter of 0.5, 0.9 and 1.4 mm than on flat glass, while it was intermediate on surfaces with beads of 2.0 and 3.1 mm in diameter (Figure 10B) (sex: $F = 5.0$; d.f. = 1, 128; $p = 0.028$; surfaces: $F = 26.8$; d.f. = 5, 128; $p < 0.001$; sex x surf.: $F = 2.3$; d.f. = 5, 128; $p = 0.052$).

Attachment ability of *A. bifasciatus* to the host eggs

The force of females is higher than that of males on the eggs of *H. halys*, whereas force values on the egg surface of *N. viridula* are similar in the two sexes (Figure 11A). The force of females is significantly higher on the eggs of *H. halys* than on the eggs of *N. viridula*, while in males there is no difference in the forces recorded on different egg surfaces (Figure 11A) (sex: $F = 13.1$; d.f. = 1, 16; surfaces: $F =$

13.1; d.f. = 1, 16; $p = 0.002$; sex x surf.: $F = 1.9$; d.f. = 1, 16; $p = 0.177$). There is no significant difference between safety factors of males and females on both egg surfaces (of *H. halys* and *N. viridula*) (Figure 11B). In females, the safety factor recorded on the egg surface of *H. halys* is higher than that recorded on *N. viridula* egg surface, while there is no difference between the safety factors recorded on both egg surfaces in males (Figure 11B) (sex: $F = 2.9$; d.f. = 1, 16; $p = 0.104$; surfaces: $F = 13.8$; d.f. = 1, 16; $p = 0.002$; sex x surf.: $F = 0.3$; d.f. = 1, 16; $p = 0.573$).

Discussion

The data collected in the present investigation reveal sexual dimorphism in the attachment devices and the attachment ability of the parasitoid *A. bifasciatus*. Males and females of this parasitoid species possess the typical Hymenoptera attachment devices represented by arolium and claws with the special features typical of Chalcidoidea (Gladun and Gumovsky,
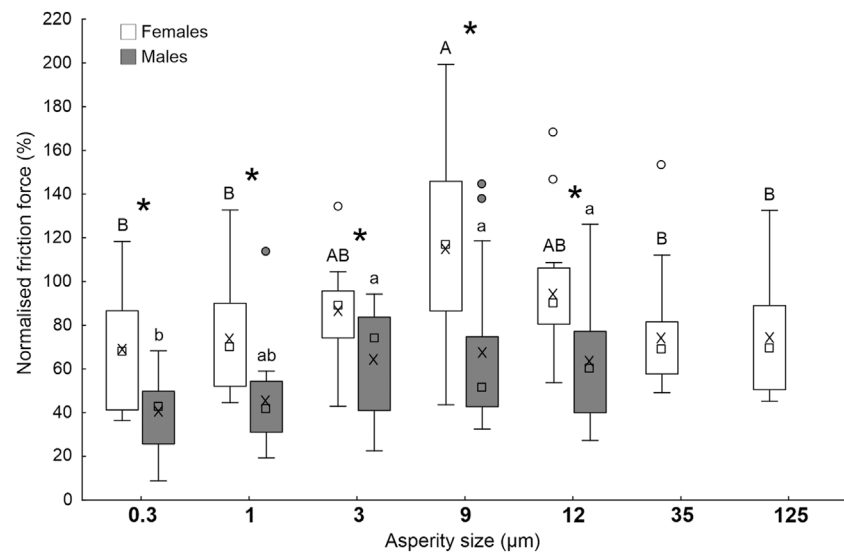
FIGURE 8
Friction force of *A. bifasciatus* females and males on polishing paper with different asperity sizes (0.3, 1, 3, 9, 12, 35 and 125 µm; 35 and 125 tested only in females), normalised to the insect friction force recorded on hydrophilic glass as reference. Boxplots show the interquartile range and the medians, whiske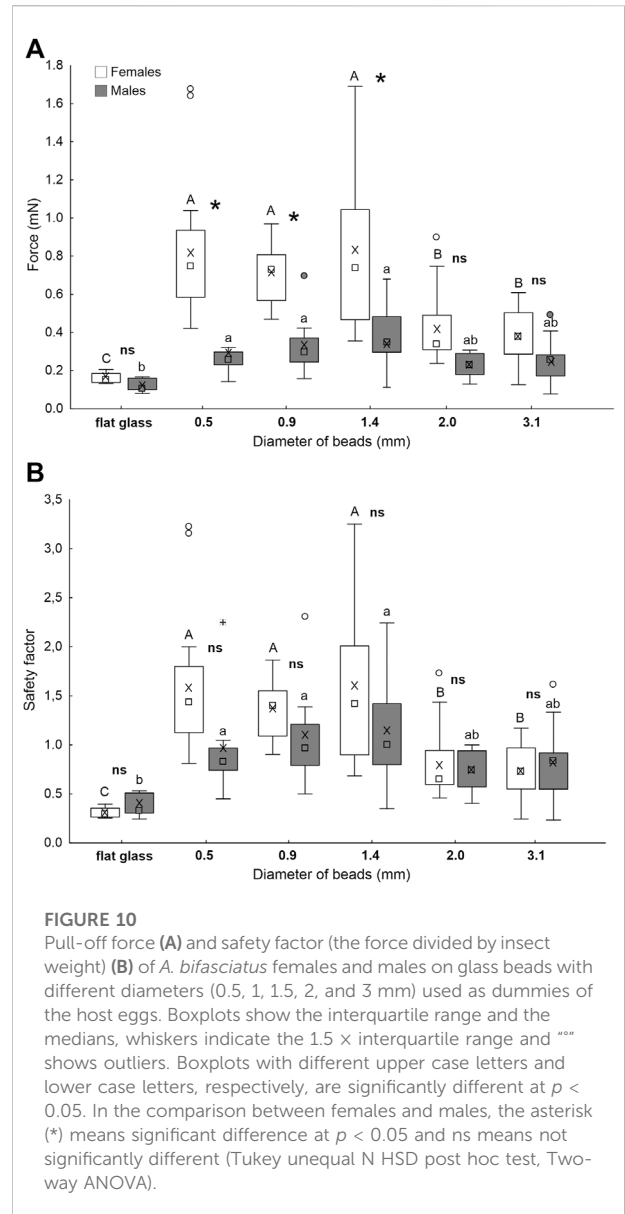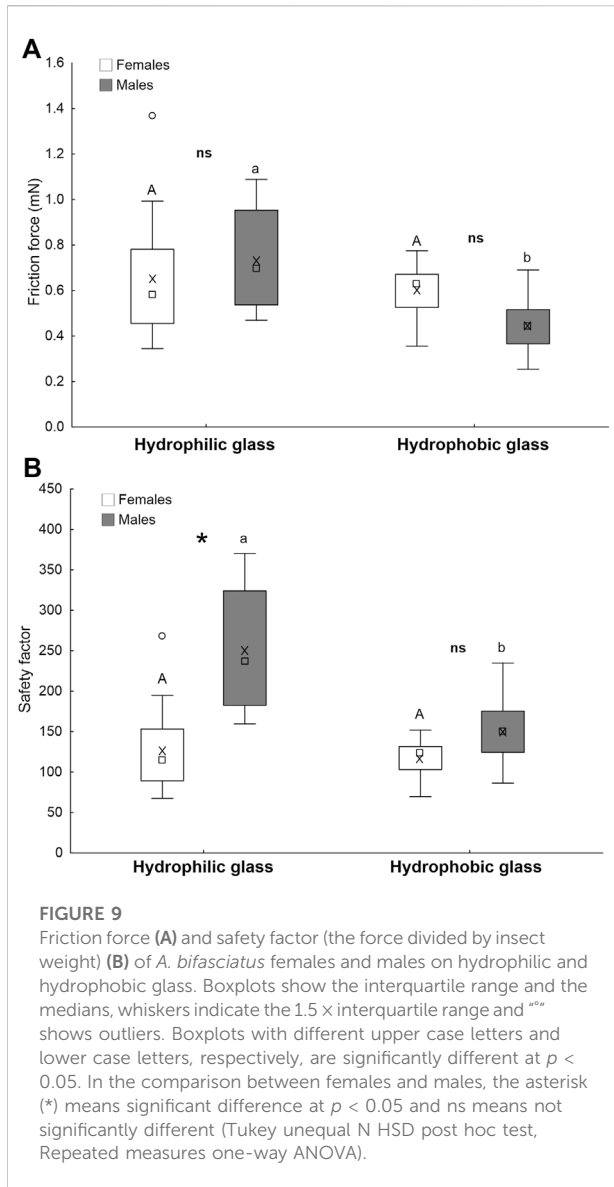rs indicate the 1.5 × interquartile range and "°" shows outliers. Boxplots with different upper case letters and lower case letters, respectively, are significantly different at $p < 0.05$ (Tukey unequal N HSD post hoc test, One-way ANOVA). In the comparison between females and males, the asterisk (*) means significant difference at $p < 0.05$ (*t*-test for independent samples).

2006). Differently from Aculeate Hymenoptera (description in Federle et al., 2001; Beutel et al., 2020), auxiliary sclerites are not present and the Chalcidoidea arolium does not fold and unfold, but rather inverts and everts (for the internal hydraulic pressure) owing to the sequential interaction of the following parts: unguitractor muscle, unguitractor plate, planta, arcus, dorsal plates, manubrium (Gladun and Gumovsky, 2006). The dorsal plates unfold laterally unrolling the planta, which allows arolium evertion (for a schematic reconstruction of the arolium eversion in Chalcidoidea see Gladun and Gumovsky, 2006). The high degree of deformability of the arolium is guaranteed by a cuticle containing a high amount of resilin (Gladun et al., 2009; Beutel et al., 2020), as typically occurs in insect attachment pads (Peisker et al., 2013; Rebora et al., 2018). Claws are short in Chalcidoidea, but can contact the surface, when they are rotated towards the first tarsomere owing to the unguitractor muscle contraction.
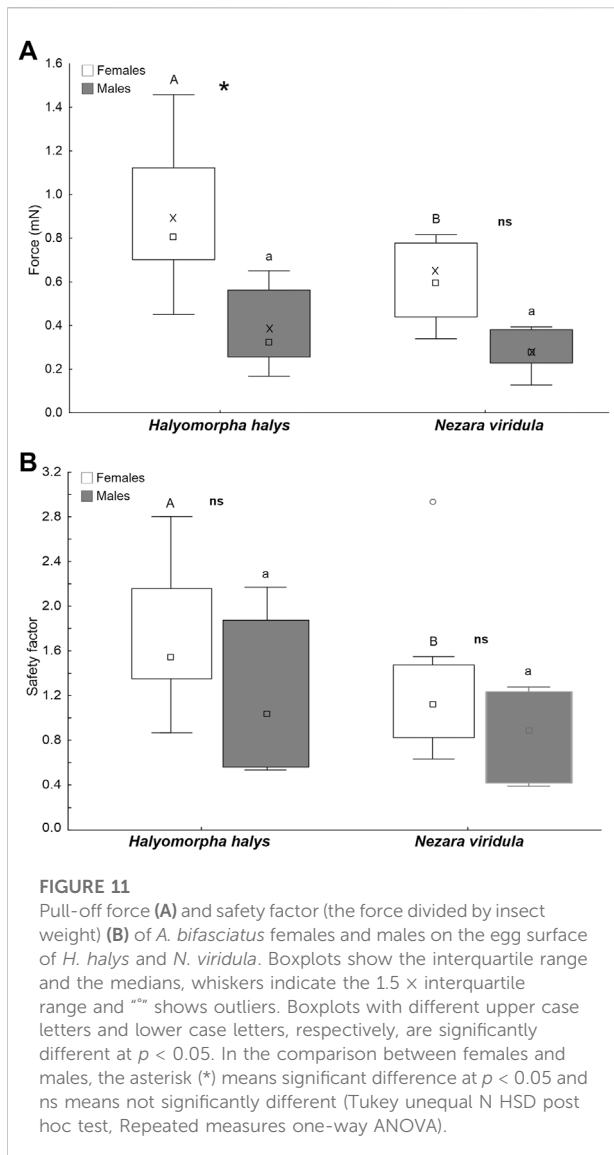
In *A. bifasciatus*, arolium and claws are similar in both sexes and differ only in their size, since females are bigger than males. The main aspect of sexual dimorphism is related to the tarsi of the midlegs. These last are completely different in the female compared to the straight tarsi of the male: they have a curved shape and the first tarsomere is wider than the others. Moreover, the female tarsomeres possess lateral rows of big and thick pegs slightly curved towards the inner portion of the tarsomere, whose number decreases from the proximal to the distal tarsomeres. Chalcidoidea insects, when moving on a flat surface, walk on

their tiptoe, using their arolia and claws. These last are effective only on rough surfaces, when the distances between adjacent asperities are larger than the claw tip diameter (Dai et al., 2002). Owing to the unguitractor muscle contraction, arolia and claws are respectively everted and rotated towards the last tarsomere (Gladun and Gumovsky, 2006). This is what can be observed in forelegs and hindlegs of an egg-laying female of *A. bifasciatus* walking on the host eggs, while a different behaviour can be described for midlegs, which are in close contact with the egg surface with the whole tarsus. Such behaviour let us hypothesize an involvement of the thick pointed pegs (and maybe also of the internal row of setae) in helping the tarsus to strongly adhere to the egg chorion. In particular, the first thick tarsomere with its high number of pegs seems to play an important role in the attachment to the egg surface. To the best of our knowledge, an involvement of these tarsal structures in the oviposition behaviour of Eupelmidae egg parasitoids has never been described. The special female midlegs with curved tarsi, thick proximal tarsomere and tarsal pegs, which are a feature typical of other representatives of the family Eupelmidae, not necessarily egg parasitoids (Gibson, 1995), have been hypothesised to contribute in preventing slipping during jumping behaviour (Gibson, 1986). Since the middle legs are the primary organs for jumping in most chalcidoids (Gibson, 1986), due to a sudden retraction of the trochanters into the coxae, which rotates the femora ventrally, straightens the femoral-tibial joints, extends the

FIGURE 9
Friction force **(A)** and safety factor (the force divided by insect weight) **(B)** of *A. bifasciatus* females and males on hydrophilic and hydrophobic glass. Boxplots show the interquartile range and the medians, whiskers indicate the 1.5 × interquartile range and "°" shows outliers. Boxplots with different upper case letters and lower case letters, respectively, are significantly different at *p* < 0.05. In the comparison between females and males, the asterisk (*) means significant difference at *p* < 0.05 and ns means not significantly different (Tukey unequal N HSD post hoc test, Repeated measures one-way ANOVA).

FIGURE 10
Pull-off force **(A)** and safety factor (the force divided by insect weight) **(B)** of *A. bifasciatus* females and males on glass beads with different diameters (0.5, 1, 1.5, 2, and 3 mm) used as dummies of the host eggs. Boxplots show the interquartile range and the medians, whiskers indicate the 1.5 × interquartile range and "°" shows outliers. Boxplots with different upper case letters and lower case letters, respectively, are significantly different at *p* < 0.05. In the comparison between females and males, the asterisk (*) means significant difference at *p* < 0.05 and ns means not significantly different (Tukey unequal N HSD post hoc test, Two-way ANOVA).

legs, and provides propulsion, the various tarsal pegs probably help the insect to attach firmly to the substrate, when the forces are exerted through the tarsus (Gibson, 1986). The role of the tarsi in jumping behaviour has been only hypothesized and further studies are necessary to clarify these aspects. Ultrastructural investigations using transmission electron microscopy could help to identify any special mechanosensory function of these structures (a chemosensory function can be excluded because on the lack of any pore on their surface). In any case, based on the data obtained in the present investigation, we can assume that the special female midleg tarsi are responsible for the good performance observed in females in centrifuge experiments on rough artificial surfaces. The force exerted by females on rough surfaces normalised to smooth surfaces is always higher than that of males and on intermediate asperity

size (9 μm) the female force is even higher than that on smooth glass. In males, whose tarsi lack these pegs, the force on rough surfaces is never higher than that recorded on smooth glass, but always considerably reduced compared to it. So, we can assume that in *A. bifasciatus* females, the presence of curved spines on the ventral tarsomeres can play a role to improve locomotion on irregular surfaces, exactly as it happens in other Hymenoptera species such as in Formicidae (Beutel et al., 2020) or in Vespidae (Frantsevich and Gorb, 2004) showing tarsi equipped with spines for a firm grip on soil or strongly sculptured plant surfaces. In this regard, we can observe that quite often insect egg surface is not smooth but decorated, as clearly seen in the chorion surface of *H. halys*, which represents one of the main hosts of *A. bifasciatus* (Roversi et al., 2016; Stahl et al., 2019; Moraglio et al., 2020;

FIGURE 11
Pull-off force **(A)** and safety factor (the force divided by insect weight) **(B)** of *A. bifasciatus* females and males on the egg surface of *H. halys* and *N. viridula*. Boxplots show the interquartile range and the medians, whiskers indicate the 1.5 × interquartile range and "°" shows outliers. Boxplots with different upper case letters and lower case letters, respectively, are significantly different at $p < 0.05$. In the comparison between females and males, the asterisk (*) means significant difference at $p < 0.05$ and ns means not significantly different (Tukey unequal N HSD post hoc test, Repeated measures one-way ANOVA).

Andreadis et al., 2021). In agreement with this, in our experiments on the egg surfaces of *H. halys* (rough surface) and *N. viridula* (less rough surface), females show higher force on the first than on the second species and on *H. halys* we observed a higher attachment ability of females compared to males. However, when considering the safety factor, the difference is not significant owing to the small male size, but in any case, the female force tends to be higher than that of males.

An interesting aspect concerning the attachment ability on eggs is related to the chorion wettability. The egg surface of the two tested host species is hydrophobic and, interestingly, when we test the female and male attachment ability on smooth hydrophilic and hydrophobic glass, we can observe that while males attach better (both in terms of friction force and safety factor) to hydrophilic glass than to hydrophobic glass, there is no difference in the attachment ability (both in terms of friction and

safety factor) to both glass samples in females. In this regard, it is important to remember that usually insects perform better on hydrophilic surfaces. A higher attachment ability on hydrophilic surfaces in comparison with hydrophobic ones has been reported in many insect species at the adult stage such as *Ceratitis capitata* Wiedemann and *Bactrocera oleae* (Rossi) (both Diptera: Tephritidae) (Salerno et al., 2020a; Rebora et al., 2020), *Acyrthosiphon pisum* Harris (Heteroptera: Aphididae) (Friedemann et al., 2015), *N. viridula* (Salerno et al., 2017), *Gastrophysa viridula* (De Geer) (Gorb and Gorb, 2009) and *Cylas puncticolis* (Boheman) (both Coleoptera: Brentidae) (Lüken et al., 2009), *Cryptolaemus montrouzieri* Mulsant (Gorb and Gorb, 2020), *Harmonia axyridis* (Pallas), *Propylea quatuordecimpunctata* (L.) (Salerno et al., 2022) and *Coccinella septempunctata* L. (all four Coleoptera: Coccinellidae) (Gorb et al., 2010; Hosoda and Gorb, 2012). A similar situation has been reported also in nymphs and larvae of different species, such as *N. viridula* (Salerno et al., 2020b), *G. viridula* (Zurek et al., 2015) and *Rhadinoceraea micans* (Schrank) (Hymenoptera: Tenthredinidae) (Voigt and Gorb, 2012). Such a decrease of the attachment ability on surfaces with increasing contact angle can be explained by the reduced role of the adhesive fluid in the generation of capillary forces, which are important for insect attachment (see review in Dirks and Federle, 2011). Examples of insects performing better on hydrophobic surfaces are not common and, when described, represent examples of insect adaptation to the host plant's surface features. This is the case of the larvae of *Galerucella nymphaea* (L.) (Coleoptera: Chrysomelidae), which show higher attachment ability to substrates with water contact angle similar to that of their host plant (80°) and lower attachment ability on substrates with higher or lower water contact angles (Grohmann et al., 2014). We can hypothesize for females of *A. bifasciatus*, a coevolution between the female attachment ability and the typical hydrophobic chorion surface, whereas coevolution is not present in the male. Further investigations on interactions between the attachment ability of other egg parasitoid species and the chemical composition of their tarsal fluid could clarify this interesting aspect.

Another aspect analysed in the present study is the attachment ability of *A. bifasciatus* to flat glass in comparison with glass beads of different sizes used as dummies of the host eggs. Our results demonstrate that adult attachment ability is higher on beads than on flat glass. This can be due to the different position of the insect on the two kinds of surfaces (simple adhesion measured on flat surfaces and adhesion plus friction measured on spherical surfaces of glass beads) and to the sexual dimorphism of midleg tarsi, which can be used on curved surfaces only by females. Interesting aspects are related to the differences observed in female and male attachment abilities: indeed, females attach more strongly than males to beads (but when considering the safety factor, the difference is non-significant owing to the small male size). Moreover, for males, the

bead diameter is not so important (there is no difference in the attachment ability to the different beads), while in females the higher attachment ability was recorded on beads with a diameter ranging from 0.5 to 1.4 mm. The diameter of the eggs of *H. halys* and that of the eggs of *N. viridula* are just in this range (about 1.28 mm in the first case and about 0.82 mm in the second case). It is unknown how females of *A. bifasciatus* can assess egg size dimension, but it is important to remember that host egg size is an essential aspect of egg parasitoid fitness. In many host-parasitoid systems, female fecundity and longevity, two extremely important parameters linked to parasitoid fitness, are positively correlated with female body size (Godfray 1994; Stahl et al., 2018). In *A. bifasciatus* females, body size and sex ratio are positively correlated to the weight (and size) of parasitized eggs (Stahl et al., 2018). On the other hand, heteropteran hosts with small eggs, such as *N. viridula*, are frequently accepted, even if only male offspring is produced (Stahl et al., 2018).

In conclusion, the data presented in this study revealed differences in the attachment devices and attachment ability between females and males of the egg parasitoid *A. bifasciatus*. We observed a special ability of the female to attach to the eggs of the two host species, thus suggesting an adaptation of the female to the surface features of the eggs during oviposition. Since in Europe *A. bifasciatus* is the most important native egg parasitoid of the eggs of the highly invasive pest species *H. halys*, studies deepening the knowledge of the interaction of this parasitoid species with its environment represent a substantial contribution to the development of biological control strategies. The deep knowledge of the mechanical interaction between the parasitoid and its host surface can help to develop artificial surfaces to improve the mass rearing technique in insectaries.

Data availability statement

The raw data supporting the conclusion of this article will be made available by the authors, without undue reservation.

Author contributions

The study was designed by all the authors. SG, MR, and GS performed the SEM investigations. GS, MR, and SP performed the force experiments. VS performed the behavioural experiments. VS and EG characterized the tested surfaces. The manuscript was written by GS and MR. All authors discussed the analysis and interpretation of the results and participated in the final editing of the manuscript.

Acknowledgments

Conflict of interest

The authors declare that the research was conducted in the absence of any commercial or financial relationships that could be construed as a potential conflict of interest.

Publisher's note

All claims expressed in this article are solely those of the authors and do not necessarily represent those of their affiliated organizations, or those of the publisher, the editors and the reviewers. Any product that may be evaluated in this article, or claim that may be made by its manufacturer, is not guaranteed or endorsed by the publisher.

References

Andreadis, S. S., Gogolashvili, N. E., Fifis, G. T., Navrozidis, E. I., and Thomidis, T. (2021). First report of native parasitoids of *Halyomorpha halys* (Hemiptera: Pentatomidae) in Greece. *Insects* 12, 984. doi:10.3390/insects12110984

Beutel, R. G., Richter, A., Keller, R. A., Garcia, F. H., Matsumura, Y., Economo, E. P., et al. (2020). Distal leg structures of the aculeata (Hymenoptera): a comparative evolutionary study of *Sceliphron* (Sphecidae) and *Formica* (Formicidae). *J. Morphol.* 281, 737–753. doi:10.1002/jmor.21133

Chiappini, E., Salerno, G., Berzolla, A., Iacovone, A., Reguzzi, C. M., and Conti, E. (2012). Role of volatile semiochemicals in host location by the egg parasitoid *Anagrus breviphragma*. *Entomol. Exp. Appl.* 144 (3), 311–316. doi:10.1111/j.1570-7458.2012.01290.x

Conti, E., and Colazza, S. (2012). Chemical ecology of egg parasitoids associated with true bugs. *Psyche* 2012, 651015. doi:10.1155/2012/651015

Conti, E., Salerno, G., Bin, F., Williams, H. J., and Vinson, S. B. (2003). Chemical cues from *Murgantia histrionica* eliciting host location and recognition in the egg parasitoid *Trissolcus brochymenae*. *J. Chem. Ecol.* 29 (1), 115–130. doi:10.1023/a:1021980614512

Dai, Z., Gorb, S. N., and Schwarz, U. (2002). Roughness- dependent friction force of the tarsal claw system in the beetle *Pachnoda marginata* (Coleoptera, Scarabaeidae). *J. Exp. Biol.* 205, 2479–2488. doi:10.1242/jeb.205.16.2479

Dirks, J-H., and Federle, W. (2011). Fluid-based adhesion in insects – principles and challenges. *Soft Matter* 7, 11047–11053. doi:10.1039/c1sm06269g

Fatouros, N. E., Cusumano, A., Bin, F., Polaszek, A., and van Lenteren, J. C. (2020). How to escape from insect egg parasitoids: a review of potential factors explaining parasitoid absence across the insecta. *Proc. R. Soc. B* 287, 20200344. doi:10.1098/rspb.2020.0344

Fatouros, N. E., Dicke, M., Mumm, R., Meiners, T., and Hilker, M. (2008). Foraging behavior of egg parasitoids exploiting chemical information. *Behav. Ecol.* 19 (3), 677–689. doi:10.1093/beheco/arn011

Federle, W., Brainerd, E. L., McMahon, T. A., and Hölldobler, B. (2001). Biomechanics of the movable pretarsal adhesive organ in ants and bees. *Proc. Natl. Acad. Sci. U. S. A.* 98 (11), 6215–6220. doi:10.1073/pnas.111139298

Frantsevich, L., and Gorb, S. (2004). Structure and mechanics of the tarsal chain in the hornet, *Vespa crabro* (Hymenoptera: Vespidae): Implications on the

attachment mechanism. *Arthropod Struct. Dev.* 33 (1), 77–89. doi:10.1016/j.asd.2003.10.003

Friedemann, K., Kunert, G., Gorb, E., Gorb, S. N., and Beutel, R. G. (2015). Attachment forces of pea aphids (*Acyrthosiphon pisum*) on different legume species. *Ecol. Entomol.* 40, 732–740. doi:10.1111/een.12249

Gibson, G. A. P. (1986). Mesothoracic skeletomusculature and mechanics of flight and jumping in eupelminae (Hymenoptera, Chalcidoidea: Eupelmidae). *Can. Entomol.* 118, 691–728. doi:10.4039/ent118691-7

Gibson, G. A. P. (1995). Parasitic wasps of the subfamily eupelminae: classification and revision of world genera (Hymenoptera: Chalcidoidea, Eupelmidae). *Mem. Entomol. Int.* 5, 421.

Gladun, D., Gorb, S. N., and Frantsevich, L. I. (2009). "Alternative tasks of the insect arolium with special reference to hymenoptera" in *Functional surfaces in biology* (Dordrecht: Springer), 67–103.

Gladun, D., and Gumovsky, A. (2006). The pretarsus in chalcidoidea (hymenoptera parasitica): functional morphology and possible phylogenetic implications. *Zool. Scr.* 35 (6), 607–626. doi:10.1111/j.1463-6409.2006.00245.x

Godfray, H. C. J. (1994). *Parasitoids, behavioural and evolutionary ecology.* Princeton, New Jersey: Princeton University Press.

Gorb, E. V., and Gorb, S. N. (2009). Effects of surface topography and chemistry of *Rumex obtusifolius* leaves on the attachment of the beetle *Gastrophysa viridula*. *Entomol. Exp. Appl.* 130 (3), 222–228. doi:10.1111/j.1570-7458.2008.00806.x

Gorb, E. V., and Gorb, S. N. (2020). Attachment ability of females and males of the ladybird beetle *Cryptolaemus montrouzieri* to different artificial surfaces. *J. Insect Physiol.* 121, 104011. doi:10.1016/j.jinsphys.2019.104011

Gorb, E. V., and Gorb, S. N. (2013). "Anti-adhesive surfaces in plants and their biomimetic potential" in *Materials design inspired by nature: function through inner architecture.* Editors P. Fratzl, J. W. C. Dunlop, and R. Weinkamer (Cambridge: The Royal Society of Chemistry), 282–309.

Gorb, E. V., and Gorb, S. N. (2009). "Functional surfaces in the pitcher of the carnivorous plant *Nepenthes alata*: a cryo-SEM approach" in *Functional surfaces in biology—adhesion related phenomena.* Editor S. N. Gorb (Dordrecht: Springer), 2, 205–238.

Gorb, E. V., Hosoda, N., Miksch, C., and Gorb, S. N. (2010). Slippery pores: antiadhesive effect of nanoporous substrates on the beetle attachment system. *J. R. Soc. Interface* 7, 1571–1579. doi:10.1098/rsif.2010.0081

Gorb, S. N., Gorb, E. V., and Kastner, V. (2001). Scale effects on the attachment pads and friction forces in syrphid flies (Diptera, Syrphidae). *J. Exp. Biol.* 204, 1421–1431. doi:10.1242/jeb.204.8.1421

Grohmann, C., Blankenstein, A., Koops, S., and Gorb, S. N. (2014). Attachment of *Galerucella nymphaeae* (Coleoptera, Chrysomelidae) to surfaces with different surface energy. *J. Exp. Biol.* 217, 4213–4220. doi:10.1242/jeb.108902

Hilker, M., and Fatouros, N. E. (2015). Plant responses to insect egg deposition. *Annu. Rev. Entomol.* 60, 493–515. doi:10.1146/annurev-ento-010814-020620

Hilker, M., and Meiners, T. (2006). Early herbivore alert: insect eggs induce plant defense. *J. Chem. Ecol.* 32 (7), 1379–1397. doi:10.1007/s10886-006-9057-4

Hosoda, N., and Gorb, S. N. (2012). Underwater locomotion in a terrestrial beetle: combination of surface de-wetting and capillary forces. *Proc. R. Soc. B* 279, 4236–4242. doi:10.1098/rspb.2012.1297

Lüken, D., Voigt, D., Gorb, S. N., and Zebitz, C. P. W. (2009). Die Tarsenmorphologie und die Haftfähigkeit des Schwarzen Batatenkäfers *Cylas puncticollis* (Boheman) auf glatten oberflächen mit unterschiedlichen physiko-chemischen Eigenschaften. *Mitt. Dtsch. Ges. Allg. Angew. Entomol.* 17, 109–113.

Moraglio, S. T., Tortorici, F., Pansa, M. G., Castelli, G., Pontini, M., Scovero, S., et al. (2020). A 3-year survey on parasitism of *Halyomorpha halys* by egg parasitoids in northern Italy. *J. Pest. Sci.* 93, 183–194. doi:10.1007/s10340-019-01136-2

Noyes, J. S. (2019). Universal Chalcidoidea database. World Wide Web Electronic publication. Available at: http://www.nhm.ac.uk/chalcidoids(Accessed March 30, 2022).

Peisker, H., Michels, J., and Gorb, S. N. (2013). Evidence for a material gradient in the adhesive tarsal setae of the ladybird beetle *Coccinella septempunctata. Nat. Commun.* 4, 1661. doi:10.1038/ncomms2576

Peri, E., Frati, F., Salerno, G., Conti, E., and Colazza, S. (2013). Host chemical footprints induce host sex discrimination ability in egg parasitoids. *PLoS One* 8 (11), e79054. doi:10.1371/journal.pone.0079054

Rebora, M., Michels, J., Salerno, G., Heepe, L., Gorb, E. V., and Gorb, S. N. (2018). Tarsal at- tachment devices of the southern green stink bug *Nezara viridula* (Heteroptera: Pentatomidae). *J. Morphol.* 279 (5), 660–672. doi:10.1002/jmor.20801

Rebora, M., Salerno, G., Piersanti, S., Gorb, E., and Gorb, S. (2020). Role of fruit epicuticular waxes in preventing *Bactrocera oleae* (Diptera: Tephritidae) attachment in different cultivars of *Olea europaea. Insects* 11 (3), 189. doi:10.3390/insects11030189

Roversi, P. F., Binazzi, F., Marianelli, L., Costi, E., Maistrello, L., and Sabbatini Pereverieri, G. (2016). Searching for native egg-parasitoids of the invasive alien species *Halyomorpha halys* (Stål) (Heteroptera: Pentatomidae) in southern Europe. *Redia* 99, 63–70. doi:10.19263/redia-99.16.01

Salerno, G., Rebora, M., Gorb, E., Kovalev, A., and Gorb, S. (2017). Attachment ability of the southern green stink bug *Nezara viridula* (Heteroptera: Pentatomidae). *J. Comp. Physiol. A* 203 (8), 601–611. doi:10.1007/s00359-017-1177-5

Salerno, G., Rebora, M., Piersanti, S., Büscher, T. H., Gorb, E. V., and Gorb, S. N. (2022). Oviposition site selection and attachment ability of *Propylea quatuordecimpunctata* and *Harmonia axyridis* from the egg to the adult stage. *Physiol. Entomol.* 47, 20–37. doi:10.1111/phen.12368

Salerno, G., Rebora, M., Piersanti, S., Gorb, E., and Gorb, S. (2020a). Mechanical ecology of fruit-insect interaction in the adult Mediterranean fruit fly *Ceratitis capitata* (Diptera: Tephritidae). *Zoology* 139, 125748. doi:10.1016/j.zool.2020.125748

Salerno, G., Rebora, M., Piersanti, S., Matsumura, Y., Gorb, E., and Gorb, S. (2020b). Variation of attachment ability of *Nezara viridula* (Hemiptera: Pentatomidae) during nymphal development and adult aging. *J. Insect Physiol.* 127, 104117. doi:10.1016/j.jinsphys.2020.104117

Salt, G. (1958). Parasite behaviour and the control of insect pests. *Endeavour* 17, 145–148. doi:10.1016/0160-9327(58)90162-5

Schmidt, J. M., and Smith, J. J. B. (1985). The mechanism by which the parasitoid wasp *Trichogramma minutum* responds to host clusters. *Entomol. Exp. Appl.* 39, 287–294. doi:10.1111/j.1570-7458.1985.tb00472.x

Schmidt, J. M. (1991). The role of physical factors in tritrophic interactions. *Redia* 74, 43–93.

Sokal, R. R., and Rohlf, F. J. (1998). *Biometry: the principles and practice of statistics in biological research.* New York, NY, USA: WH Freeman and Company, 887.

Stahl, J. M., Babendreier, D., and Haye, T. (2019). Life history of *Anastatus bifasciatus*, a potential biological control agent of the Brown marmorated stink bug in Europe. *Biol. Control* 129, 178–186. doi:10.1016/j.biocontrol.2018.10.016

Stahl, J. M., Babendreier, D., and Haye, T. (2018). Using the egg parasitoid *Anastatus bifasciatus* against the invasive Brown marmorated stink bug in Europe: can non-target effects be ruled out? *J. Pest Sci.* 91, 1005–1017. doi:10.1007/s10340-018-0969-x

StatSoft Inc. (2001). *Statistica (data analysis software system) version 6 StatSoft italia SRL vigonza (PD).* Italy: StatSoft Inc., 26.

Strand, M. R., and Vinson, S. B. (1983). Analyses of an egg recognition kairomone of *Telenomus heliothidis* (Hymenoptera: Scelionidae) isolation and host function. *J. Chem. Ecol.* 9 (3), 423–432. doi:10.1007/bf00988459

van Lenteren, J. C., Bolckmans, K., Köhl, J., Ravensberg, W. J., and Urbaneja, A. (2018). Biological control using invertebrates and microorganisms: plenty of new opportunities. *BioControl* 63, 39–59. doi:10.1007/s10526-017-9801-4

Vinson, S. B. (1998). The general host selection behavior of parasitoid Hymenoptera and a comparison of initial strategies utilized by larvaphagous and oophagous species. *Biol. Control* 11, 79–96. doi:10.1006/bcon.1997.0601

Voigt, D., and Gorb, S. N. (2012). Attachment ability of sawfly larvae to smooth surfaces. *Arthropod Struct. Dev.* 41, 145–153. doi:10.1016/j.asd.2011.10.001

Zurek, D. B., Gorb, S. N., and Voigt, D. (2015). Locomotion and attachment of leaf beetle larvae *Gastrophysa viridula* (Coleoptera, Chrysomelidae). *Interface Focus* 5, 20140055. doi:10.1098/rsfs.2014.0055